Published in final edited form as:
Small. 2010 July 19; 6(14): 1492–1498. doi:10.1002/smll.201000544.

Uniform Beads with Controllable Pore Sizes for Biomedical Applications**

Sung-Wook Choi[†],
Department of Biomedical Engineering, Washington University, St. Louis, Missouri 63130 (USA)

Yi-Chun Yeh[†],
Department of Biomedical Engineering, Washington University, St. Louis, Missouri 63130 (USA)

Department of Chemical Engineering, National Tsing Hua University, Hsinchu, Taiwan (R.O.C.)

Yu Zhang,
Department of Biomedical Engineering, Washington University, St. Louis, Missouri 63130 (USA)

Hsing-Wen Sung[Prof.], and
Department of Chemical Engineering, National Tsing Hua University, Hsinchu, Taiwan (R.O.C.)

Younan Xia[*]**[Prof.]**
Department of Biomedical Engineering, Washington University, St. Louis, Missouri 63130 (USA)

Abstract

Uniform, porous poly(D, L-lactide-*co*-glycolide) (PLGA) beads with controllable pore sizes were prepared using an unstable water-in-oil (W-O) emulsion and a simple fluidic device. Optical micrographs revealed that the unstable emulsion phase-separated into two phases: the top layer rich in large water droplets and the bottom layer rich in small water droplets. When a syringe with a luer tip offset from the barrel was used, we could selectively introduce each layer of the phase-separated emulsion as a discontinuous phase into the fluidic device while a poly(vinyl alcohol) (PVA) solution was used as the continuous phase. The resultant water-in-oil-in-water (W-O-W) droplets evolved into PLGA beads with pores both in the interior and on the surface after the organic solvent had evaporated. Porous beads prepared using the top layer exhibited larger pores and windows interconnecting the pores than the beads obtained from the bottom layer. To show the effect of pore size on cell growth, we cultured fibroblasts in the beads with small and large pores. Fluorescence micrographs and 3-(4,5-dimethylthiazol-2-yl)-2,5-diphenyltetrazolium bromide (MTT) assay confirmed a high density of viable cells in the beads with large pores. These results suggest that the beads with large pores could provide a more favorable environment for cells and thus be potentially useful for tissue engineering and cell delivery applications.

Keywords

fluidic device; porous bead; phase-separated emulsion; cell viability

**This work was supported in part by an NIH Director's Pioneer Award (5DP1 OD000798) and startup funds from Washington University in St. Louis. Part of the work was done at the Nano Research Facility (NRF), a member of the National Nanotechnology Infrastructure Network (NNIN), which is supported by the NSF under ECS-0335765. S.W.C. was also partially supported by a postdoctoral fellowship from Korea Research Foundation Grant funded by the Korean Government (KRF-2007-357- D00080). Y.C.Y. was also partially supported by a grant from the National Science Council (NSC 98-2120-M-007-007).

[*]xia@biomed.wustl.edu.
[†]These two authors contributed equally to this work.

Three-dimensional biodegradable porous matrices have been of great interest for biomedical applications. So far, many investigations have been conducted for developing successful scaffold systems capable of providing an optimal environment for cells, eventually for the regeneration of a specific tissue or organ. It has been reported that cell necrosis often occurs due to the insufficient supply of nutrients/oxygen and the accumulation of metabolic wastes, especially in the center of a large scaffold.[1–4] In order to address this problem, bioreactors and hydrogels were developed to enhance the transportation of oxygen/nutrients and metabolic wastes. However, due to excessive shear stress, cell viability still needs to be greatly improved for the bioreactor systems.[5–9] In addition, hydrogels have intrinsic shortcomings, including low mechanical strength and durability. As an alternative, solid beads have been introduced to overcome these problems.[10,11] More recently, several groups demonstrated that porous beads could provide a better environment for cells in terms of viability, cell morphology, and phenotypic expression level as compared to the solid beads.[12–14]

Porous beads are attractive for applications in tissue engineering and cell delivery due to their high porosity and large surface areas for cell attachment/growth, as well as the injectability of cell/bead constructs into the body using a needle without surgical operation. To this end, a variety of porous beads made of different materials have been used as building blocks for constructing large tissues by agglomerating the cell/bead constructs in molds with specific shapes,[10,15,16] and cell delivery carriers for reconstructing a damaged tissue or organ by directly injecting the therapeutic cell/bead constructs into a damaged site.[17–20] The advantages of porous beads include large surface area, good mechanical strength, and high interconnectivity; all of them could facilitate cell seeding and migration, as well as transportation of nutrient/oxygen and metabolic wastes, in addition to the protection of cells in porous beads from physical damages. A number of techniques have been demonstrated for producing the porous beads.[2,13–14,17–20] However, most of these methods were mainly based on the use of a gas forming agent and the resultant beads were often limited in terms of structure openness and interconnectivity, porosity, and especially size uniformity for the beads.

Based on emulsion-templating, here we demonstrate a simple method for fabricating uniform porous beads with different pore sizes using a simple fluidic device fabricated from a glass capillary tube, a needle, and a poly(vinyl chloride) (PVC) tube. In our approach, an unstable water-in-oil (W-O) emulsion, being in the course of phase-separation, was introduced into the fluidic device as a discontinuous phase while an aqueous solution of poly(vinyl alcohol) (PVA) served as the continuous phase. By selectively injecting different portions of the phase-separated emulsion into the fluidic device, we could obtain porous beads with small and large pores both in the interior and on the surface. The aim of this work is to demonstrate the effect of pore size on cell growth by culturing cells in beads with small or large pores.

The primary W-O emulsion was prepared by homogenizing an aqueous solution of gelatin (7.5 wt%) and PVA (1 wt%) in a poly(D, L-lactide-*co*-glycolide) (PLGA) solution (2 wt%) without any oil-soluble surfactant. A turbid liquid phase was observed at the bottom of the W-O emulsion, together with a yellowish liquid phase at the top due to the color of gelatin solution. To monitor phase separation over time, we took photographs of the W-O emulsion hosted in a vial after homogenization. As shown in Figure 1A, the W-O emulsion without the oil-soluble surfactant became unstable just after homogenization and completely phase-separated in 10 min, whereas the W-O emulsion with an oil-soluble surfactant showed moderate stability. The degrees of phase separation in both the emulsions were quantitatively evaluated by measuring the height of the top layer of the emulsion over time (Figure 1B). We compared four different W-O emulsions: aqueous solution of gelatin (7.5

wt%) and PVA (1 wt%) in PLGA (2 wt%) solution with (3 wt%) and without Span® 80, and aqueous PVA (1 wt%) solution in PLGA (2 wt%) solution with (3 wt%) and without Span® 80. As shown in Figures 1 and S1, the emulsions consisting of PVA, PLGA and Span® 80 showed the highest emulsion stability among these samples, clearly indicating that the absence of an oil-soluble surfactant was largely responsible for the phase separation.

Figure 2, A and B, shows schematic diagrams of the fluidic device with two flow channels for producing uniform water-in-oil-in-water (W-O-W) droplets. We could selectively introduce the bottom (Figure 2A) or top (Figure 2B) layer of the phase-separated emulsion into the fluidic device using a syringe with a luer tip offset from the center of the barrel. Figure 2, C and D, shows optical micrographs taken from the bottom and top layers of the emulsion, where the gelatin/water droplets were dispersed in an oil phase. Small gelatin/water droplets were mainly found in the bottom layer of the emulsion at a low volume ratio relative to the oil phase, whereas the large, coalesced gelatin/water droplets dominated the top layer at a high volume ratio. This observation could be ascribed to the high density of DCM (1.33 g/cm^3) and the absence of an oil-soluble surfactant. We also observed that the gelatin/water droplets dispersed in the oil phase gradually coalesced over time, leading to an increase in size for the droplets. The W-O emulsion, when selectively introduced into the fluidic device, evolved into W-O-W droplets at the tip of the needle due to the flowing continuous phase. The resultant W-O-W droplets were subsequently solidified via solvent extraction and evaporation in a collection phase (water), generating porous beads. The collection phase was cooled to 4 °C with an ice bath prior to the formation of W-O-W droplets. Note that the gelatin/water droplets dispersed in the oil phase remained in the soft gel state due to the high concentration (7.5 wt%) of gelatin,[21] supporting the emulsion structure even in the course of solvent evaporation. By contrast, without the use of an ice bath, we obtained porous beads with pores less than 20 μm in diameter, even when the top layer of the W-O emulsion was employed. The reduction in pore size can be attributed to the diffusion of gelatin from the water droplets into the continuous or collection phase during solvent evaporation.

When the syringe tip was placed at the lower position, the emulsion rich in small water droplets was introduced into the fluidic device, eventually leading to beads with small pores due to the small sizes of the water droplets, and vice versa. Figure 3 shows optical micrographs and SEM images of porous beads with uniform diameters and a spherical shape. It is clear that the beads prepared using the top layer of the unstable emulsion exhibited much larger sizes for both pores and windows interconnecting the pores, as compared to the beads prepared using the bottom layer of the emulsion. In addition, the perimeter of the bead with large pores was mostly occupied by the pores, whereas the bead with small pores had a large surface area at the perimeter. The average diameters of the beads with small and large pores were 321.5 ± 12.6 (coefficient of variation or CV: 3.92%) and 368.5 ± 9.6 (CV: 2.61%) μm, respectively. These characteristics are consistent with the structures of the W-O emulsion, the high volume ratio of the gelatin/water droplets to the oil phase, and the large diameter of the coalesced gelatin/water droplets. When an aqueous PVA (1 wt%) solution was emulsified in a PLGA (2 wt%) solution with Span® 80 surfactant (3 wt%), the emulsion stability was remarkably enhanced (Figure S1), and the resultant beads prepared from the stable emulsion only showed surface pores less than 10 μm in diameter (Figure S2).

Figure 4, A and B, shows the size distributions of surface and inner pores for the beads with small and large pores. The average sizes of the surface pores for the beads with small and large pores were 13.1 ± 7.3 and 35.8 ± 12.5 μm, respectively. By considering the typical dimensions of a cell, there should be a small chance for a cell to penetrate into the bead with surface pores less than 20 μm during cell seeding. Therefore, in the case of the beads with

small pores, 21% of the surface pores with diameters >20 μm are critical for cell penetration into the beads. By contrast, most of the surface pores on the beads with large pores are well-suited for cell penetration. The average sizes of the inner pores for the beads with small and large pores were determined to be 16.2 ± 7.4 and 46.8 ± 9.3 μm, respectively. The larger size of the inner pores than the surface pores could be attributed to the gradual coalescence of the gelatin/water droplets in the course of solidification. Besides pores, the window interconnecting pores also plays an important role in cell survival because it serves as a route for cell migration and transportation of nutrients/oxygen. Most of the windows for the beads with small and large pores were in the ranges of 1 to 10 and 20 to 40 μm, respectively (Figure 4C).

We then demonstrated the potential use of the porous beads for biomedical applications by culturing NIH-3T3 fibroblasts in them. The beads with different pore sizes were compared in terms of cell penetration, growth, and viability after seeding and then culture for different periods of time. Prior to cell seeding, the beads were incubated in a serum-containing medium overnight to allow certain proteins in the serum to adsorb onto the surface of the beads and thus facilitate cell attachment via integrin receptors.[20,22] The cells were seeded on each types of bead with different pore sizes and cultured in a spinner flask with gentle stirring at 50 rpm for 24 h. Fluorescence microscopy and 3-(4,5-dimethylthiazol-2-yl)-2,5-diphenyltetrazolium bromide (MTT) assay were used to follow the attachment and proliferation of the cells in the beads.

Figure 5A shows fluorescence micrographs of microtomed sections of the cell/bead constructs after 1 day of culture. Interestingly, despite the limited number of large surface pores (>20 μm in diameter) for the beads with small pores, several cells were observed at the center of the bead. It is likely that suspended cells (around 10 μm in diameter, Figure S3) could reach the center of the bead through some of the large pores and windows during cell seeding. It appeared that more cells could penetrate and reach the center for the beads with large pores than those with small pores. This could be ascribed to the high percentage ratio of large surface pores and windows for the beads with large pores. Quantitative analysis of cell density as a function of distance from the center of the bead indicates that most of the cells were crowded around the perimeter of the bead with small pores whereas the cells in the bead with large pores were relatively well distributed throughout the bead (Figure 5B).

The cells in the beads were incubated for up to 10 days and the number of viable cells in each sample was evaluated by MTT assay. As shown in Figure 6A, the proliferation rate of cells in the beads with small pores was slightly faster than in the beads with large pores up to 5 days of culture, which is probably due to the large outer surface area of the beads with small pores. However, the cells cultured in the beads with small pores dramatically lost their viability after 7 days of culture, whereas the cells in the beads with large pores kept growing slowly with high viability. We also conducted live/dead staining to distinguish live and dead cells with different colors. As shown in Figure 6B, fluorescence micrographs of cell/bead construct confirmed the high cell viability in the beads with large pores.

The difference in cell viability can be explained as follows. As shown in Figure 7A, some of the pores (~10 μm) in the bead with small pores were blocked by the stretched cells (typically >20 μm in size, Figure S3) and secreted extracellular matrix even at 1 day of culture. This would lead to a limited transportation of nutrients/oxygen and eventually cell death in the central region of the bead.[23–29] It is expected that the small windows (<10 μm) can also be easily blocked by the cells. Moreover, the bead with small pores was surrounded by a cell layer at 7 days of culture because the large outer surface area at the perimeter of the beads could support the cell growth (Figure 7B). This cell layer could consume a majority of nutrients/oxygen and physically restrict the transportation of

nutrients/oxygen into the interior of the bead. These results suggested that the size of pores and windows, as well as the surface area at the perimeter of the bead, are all important factors in determining cell viability. For practical applications in tissue engineering and cell delivery, the uniformity in overall diameter for the beads might allow for a precise control over the amount of cells, relative to non-uniform porous beads. In addition, the overall diameter of the beads can be easily tuned by changing the flow rate of each phase and dimensions of the fluidic device without destroying the uniformity in bead diameter.[30] We can also make much smaller beads with diameters around 100 μm using needles and glass capillaries with smaller dimensions.

In summary, we have successfully fabricated uniform beads with small or large pore sizes using a simple fluidic device. The employment of an unstable emulsion and the use of a syringe with a tip offset from the center of barrel allowed us to control the pore size of the resultant beads. By introducing the top layer of emulsion rich in large water droplets into the fluidic device, we could obtain uniform beads with large pores and windows. High viability and loading of cells in the beads with large pores were also confirmed by culturing fibroblasts, compared to the beads with small pores. Despite the high cell viability for beads with large pores, many other parameters also need to be considered and optimized in the future work, including, for example, cell type and cell-cell interaction,[31] mechanical strength, and the overall diameter of the beads. We believe that the uniform, porous beads have great potential for applications in tissue engineering and cell delivery. In the next step, our goal will be focused on the formation of large and thick tissue using the beads as building blocks and also the development of therapeutic cell delivery systems capable of injecting cell/bead construct into a body.

Experimental Section

Materials

Poly(D, L-lactide-*co*-glycolide) (PLGA, 75:25, M_w≈66,000–107,000, Sigma), Gelatin (Type A, from porcine skin, Sigma-Aldrich), poly(vinyl alcohol) (PVA, M_w≈13,000–23,000, 98% hydrolyzed, Aldrich), and Span® 80 (Sigma) were used for fabricating porous beads. Dichloromethane (DCM, ≥99.5%, Sigma) served as an organic solvent for PLGA. The glass capillary tubes were purchased from Ace Glass. The water used in all experiments was obtained by filtering through a set of Millipore cartridges (Epure, Dubuque, IA).

Emulsion stability test

Four different emulsions were tested to understand the instability of the emulsions: an aqueous solution (2 g) of gelatin (7.5 wt%) and PVA (1 wt%) in 6 g of a PLGA solution (2 wt%), with (3 wt%) or without Span® 80; and an aqueous solution (2 g) of PVA (1 wt%) in 6 g of a PLGA solution (2 wt%), with (3 wt%) or without Span® 80. Photographs of each emulsion in a vial were taken over time after homogenization at 20,000 rpm for 3 min. The height of the top layer of each emulsion was measured from the photograph and normalized to the total height of the mixture.

Preparation and characterization of porous beads using a fluidic device

The fluidic device consisted of poly(vinyl chloride) (PVC) tube (1/32 in. i.d. × 3/32 in. o.d.), a glass capillary (0.5 mm i.d. × 0.9 mm o.d.), and a 26G needle. The device with two way flow channels was fabricated by inserting the needle and the capillary tube into the PVC tube, followed by sealing with epoxy adhesive.[30] The W-O emulsion was prepared by emulsifying an aqueous solution (2 g) of gelatin (7.5 wt%) and PVA (1 wt%) in 6 g of a PLGA solution (2 wt%) with a homogenizer (Dispenser T 10 basic, IKA® works, Inc.) at 20,000 rpm for 3 min. In 5 min after homogenization, the W-O emulsion was introduced as

a discontinuous phase into the fluidic device, where an aqueous PVA solution (1 wt%) served as the continuous phase. A syringe with a luer tip offset from the center of the barrel was employed to selectively introduce the top or bottom layer of the phase-separated emulsion (Figure 2). The production of could continuously run until most of the emulsion in each layer had been injected into the fluidic device. The flow rates for the discontinuous and continuous phases were kept at 0.05 and 2 mL/min, respectively. Water-in-oil-in water (W-O-W) droplets, formed at the tip of the needle, flowed along the capillary tube into a 1-L tall beaker containing 900 mL of water (the collection phase) placed in an iced bath and gently stirred overnight to allow the organic solvent to dissipate into the collection phase and then evaporate. Afterwards, the resultant beads with gelatin were immersed into 900 mL of warm water held at 45 °C under gentle stirring for 3 h to completely remove residual gelatin and then washed with water three times.

Optical/fluorescence microscopy (Axioskop 2, Carl Zeiss) and scanning electron microscopy (SEM, Nova NanoSEM 2300, FEI) were used to characterize the W-O emulsions and the resultant beads. The average diameters and standard deviations for inner and surface pores, and windows between the pores were calculated from SEM images by analyzing at least 5 beads for each sample using ImageJ software (National Institutes of Health, USA).

In vitro cell culture

To investigate cell growth in the porous beads, NIH-3T3 fibroblast (ATCC, American Type Culture Collection, Manassas, VA) was used as a model system. Prior to cell seeding, porous beads with different pore sizes were sterilized by immersion in 70% ethanol overnight, and subsequently washed with PBS three times. After removing PBS, the porous beads were resuspended in culture medium including 50% normal calf serum (NCS, ATCC) at 37 °C overnight, and then washed with PBS three times. For cell seeding, 4×10^5 cells in 40 mL of culture media were incubated with roughly 100 porous beads in a spinner flask with gentle stirring at 50 rpm for 24 h. After incubation, the porous beads containing cells were washed with PBS three times to remove loosely attached cells, and then transferred into a 96-well culture plate (one porous bead per well). The culture medium consisted of DMEM (Invitrogen Corp. Grand Island, NY) supplemented with 10% NCS and 1% antibiotics (containing penicillin and streptomycin, Invitrogen). The culture was maintained at 37 °C in a humidified atmosphere containing 5% CO_2 and the medium was changed every other day.

Cell viability test

Cell viability was measured by 3-(4,5-dimethylthiazol-2-yl)-2,5-diphenyl tetrazolium bromide (MTT) assay (Invitrogen), which is based on the metabolic conversion of the tetrazolium salt into purple formazan to be measured photospectrometrically. After harvesting the cells at 1, 3, 5, 7 and 10 days of culture, the medium was removed, 270 μL fresh medium and 30 μL MTT (5 mg/mL in PBS) were added to each well, and incubated at 37 °C, 5% CO_2 for 3 h. After removing the medium, the formazan was dissolved with 2-propanol (Sigma). Absorbance at 560 nm was measured using a microplate reader (TECAN, USA). The cell viability in the porous beads with different pore sizes was also investigated using a fluorescence microscope by LIVE/DEAD® assay (Invitrogen). After harvesting the cells at 10 days of culture, the medium was removed, washed with PBS two times, and then resuspended in PBS containing 2 μM calcein AM and 4 μM ethidium homodimer, according to the manufacturer's instruction, at 37 °C for 40 min.

To observe cell distribution in porous beads, porous beads containing cells were fixed in 3.7% formaldehyde solution in PBS for 15 min, washed with PBS three times, and then

stored in PBS. The beads with cells were sliced into sections of 20 μm in thickness using microtome (Microm HN505E, Cryostat) and then the sections were stained with 4,6-diamino-2-phenylindole (DAPI, Invitrogen) for nucleus. The sections were examined using a fluorescence microscope (Axioskop 2, Carl Zeiss). The distribution of the cells in the bead was calculated from the fluorescence micrographs by measuring the distances of the cells from the center of the bead using ImageJ software.

Supplementary Material

Refer to Web version on PubMed Central for supplementary material.

References

1. Yang J, Yamato M, Kohno C, Nishimoto A, Sekine H, Fukai F, Okano T. Biomaterials. 2005; 26:6415. [PubMed: 16011847]
2. Lim SM, Lee HJ, Oh SH, Kim JM, Lee JH. J. Biomed. Mater. Res. B. 2009; 90:521.
3. Ma PX, Zhang R, Xiao G, Franceschi R. J. Biomed. Mater. Res. A. 2001; 54:284.
4. Sikavitsas VI, Bancroft GN, Mikos AG. J. Biomed. Mater. Res. 2002; 62:136. [PubMed: 12124795]
5. Goldstein AS, Juarez TM, Helmke CD, Gustin MC, Mikos AG. Biomaterials. 2001; 22:1279. [PubMed: 11336300]
6. Fuchs JR, Terada S, Hannouche D, Ochoa ER, Vacanti JP, Fauza DO. J. Pediatr. Surg. 2002; 37:1720. [PubMed: 12483640]
7. Martin I, Wendt D, Heberer M. Trends Biotechnol. 2004; 22:80. [PubMed: 14757042]
8. Gooch KJ, Kwon JH, Blunk T, Langer R, Freed LE, Vunjak-Novakovic G. Biotechnol. Bioeng. 2001; 72:402. [PubMed: 11180060]
9. Croughan MS, Hamel JF, Wang DIC. Biotechnol. Bioeng. 1987; 29:130. [PubMed: 18561137]
10. Sahoo SK, Panda AK, Labhasetwar V. Biomacromolecules. 2005; 6:1132. [PubMed: 15762686]
11. Senuma Y, Franceschin S, Hilborn JG, Tissières P, Bisson I, Frey P. Biomaterials. 2000; 21:1135. [PubMed: 10817266]
12. Kang SW, La WG, Kim BS. J. Biomater. Sci. Polym. Ed. 2009; 20:399. [PubMed: 19192363]
13. Chung HJ, Park TG. Tissue Eng A. 2009; 15:1391.
14. Chung HJ, Kim IK, Kim TG, Park TG. Tissue Eng A. 2008; 14:607.
15. Furukawa KS, Miyauchi S, Suzuki D, Umezu Y, Shinjo T, Ushida T, Eguchi M, Tateishi T. Mater. Sci. Eng. C. 2004; 24:437.
16. Matsuno T, Hashimoto Y, Adachi S, Omata K, Yoshitaka Y, Ozeki Y, Umezu Y, Tabata Y, Nakamura M, Satoh T. Dent. Mater. J. 2008; 27:827. [PubMed: 19241692]
17. Senuma Y, Franceschin S, Hilborn JG, Tissières P, Bisson I, Frey P. Biomaterials. 2000; 21:1135. [PubMed: 10817266]
18. Eiselt P, Yeh J, Latvala RK, Shea LD, Mooney DJ. Biomaterials. 2000; 21:1921. [PubMed: 10941913]
19. McGlohorn JB, Grimes LW, Webster SS, Burg KJL. J. Biomed. Mater. Res. A. 2003; 66:441. [PubMed: 12918025]
20. Kim TK, Yoon JJ, Lee DS, Park TG. Biomaterials. 2006; 27:152. [PubMed: 16023197]
21. Tosh SM, Marangoni AG. Appl. Phys. Lett. 2004; 84:4242.
22. Krebs MD, Sutter KA, Lin AS, Guldberg RE, Alsberg E. Acta Biomater. 2009; 5:2847. [PubMed: 19446056]
23. Oh SH, Park IK, Kim JM, Lee JH. Biomaterials. 2007; 28:1664. [PubMed: 17196648]
24. Melero-Martin JM, Dowling MA, Smith M, Al-Rubeai M. Biomaterials. 2006; 27:2970. [PubMed: 16455134]
25. Carmeliet P, Jain RK. Nature. 2000; 407:249. [PubMed: 11001068]
26. Lin RZ, Chang HY. Biotechnol. J. 2008; 3:1172. [PubMed: 18566957]

27. Curcio E, Salerno S, Barbieri G, De Bartolo L, Drioli E, Bader A. Biomaterials. 2007; 28:5487. [PubMed: 17881050]
28. Lee WY, Chang YH, Yeh YC, Chen CH, Lin KM, Huang CC, Chang Y, Sung HW. Biomaterials. 2009; 30:5505. [PubMed: 19631978]
29. Glicklis R, Merchuk JC, Cohen S. Biotechnol. Bioeng. 2004; 86:672. [PubMed: 15137079]
30. Choi SW, Cheong IW, Kim JH, Xia Y. Small. 2009; 5:454. [PubMed: 19189332]
31. Shi X, Sun L, Jiang J, Zhang X, Ding W, Gan Z. Macromol. Biosci. 2009; 9:1211. [PubMed: 19821453]

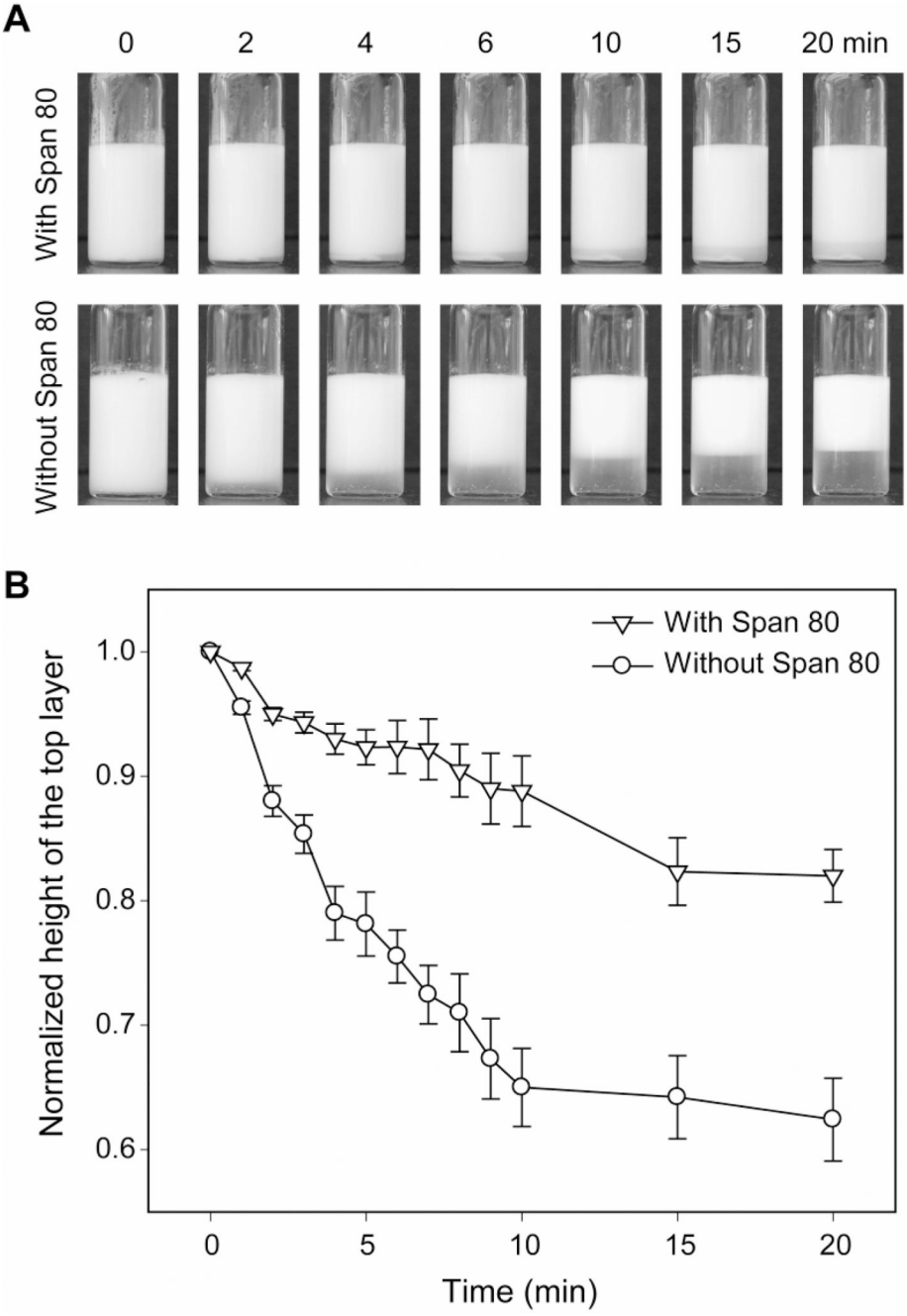

Figure 1.

A) Photographs of W-O emulsions showing phase separation over time. An aqueous solution of gelatin (7.5 wt%) and PVA (1 wt%) was emulsified in a PLGA (2 wt%) solution with or without Span® 80 (3 wt%). B) Quantitative analysis of the height of the top layer of the emulsions. The height of the top layer was normalized against the total height of the emulsion.

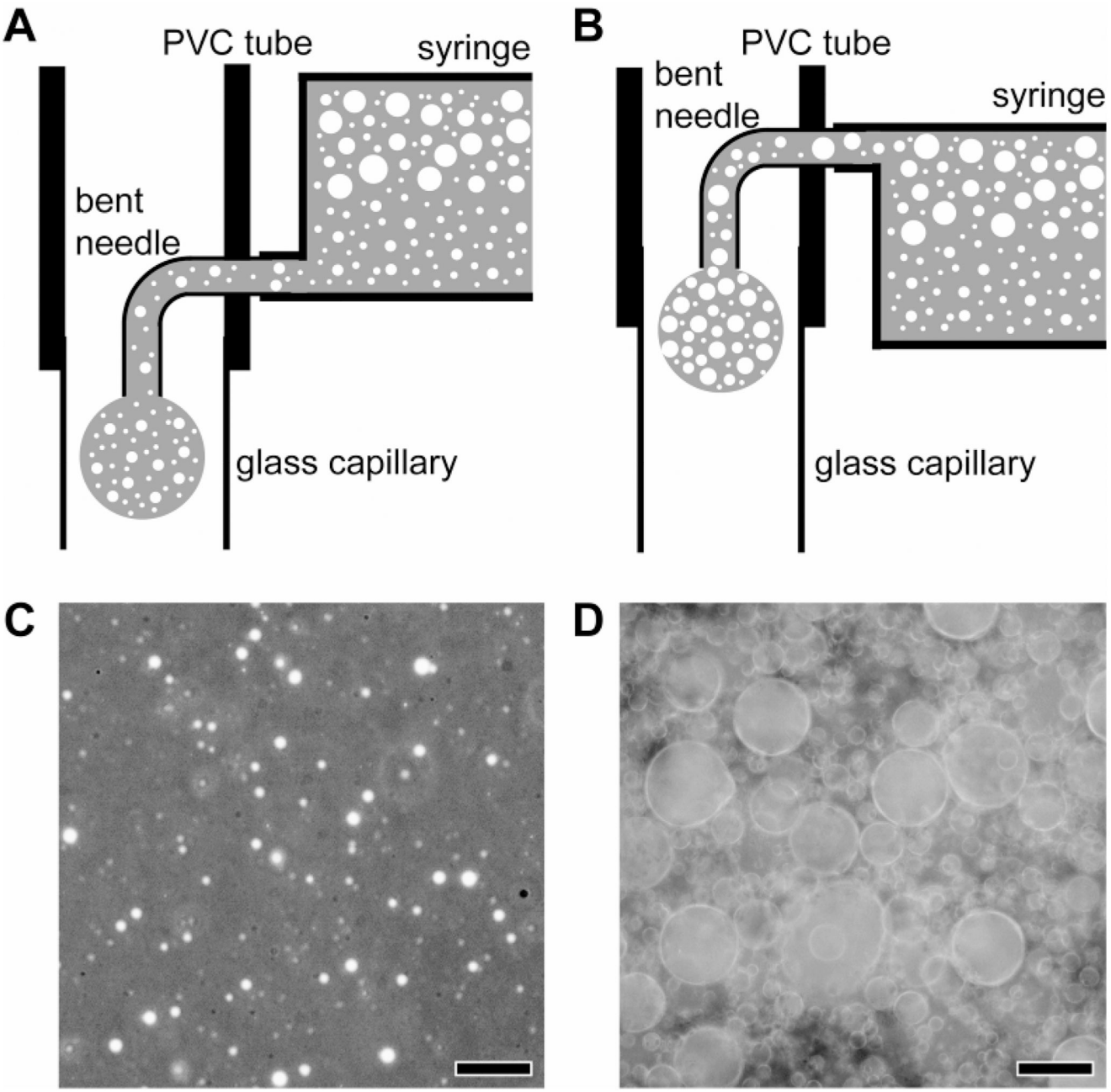

Figure 2.
A, B) Schematic diagrams of the fluidic devices and optical micrographs of C) the bottom layer and D) the top layer of the phase-separated emulsion. The scale bars are 10 μm.

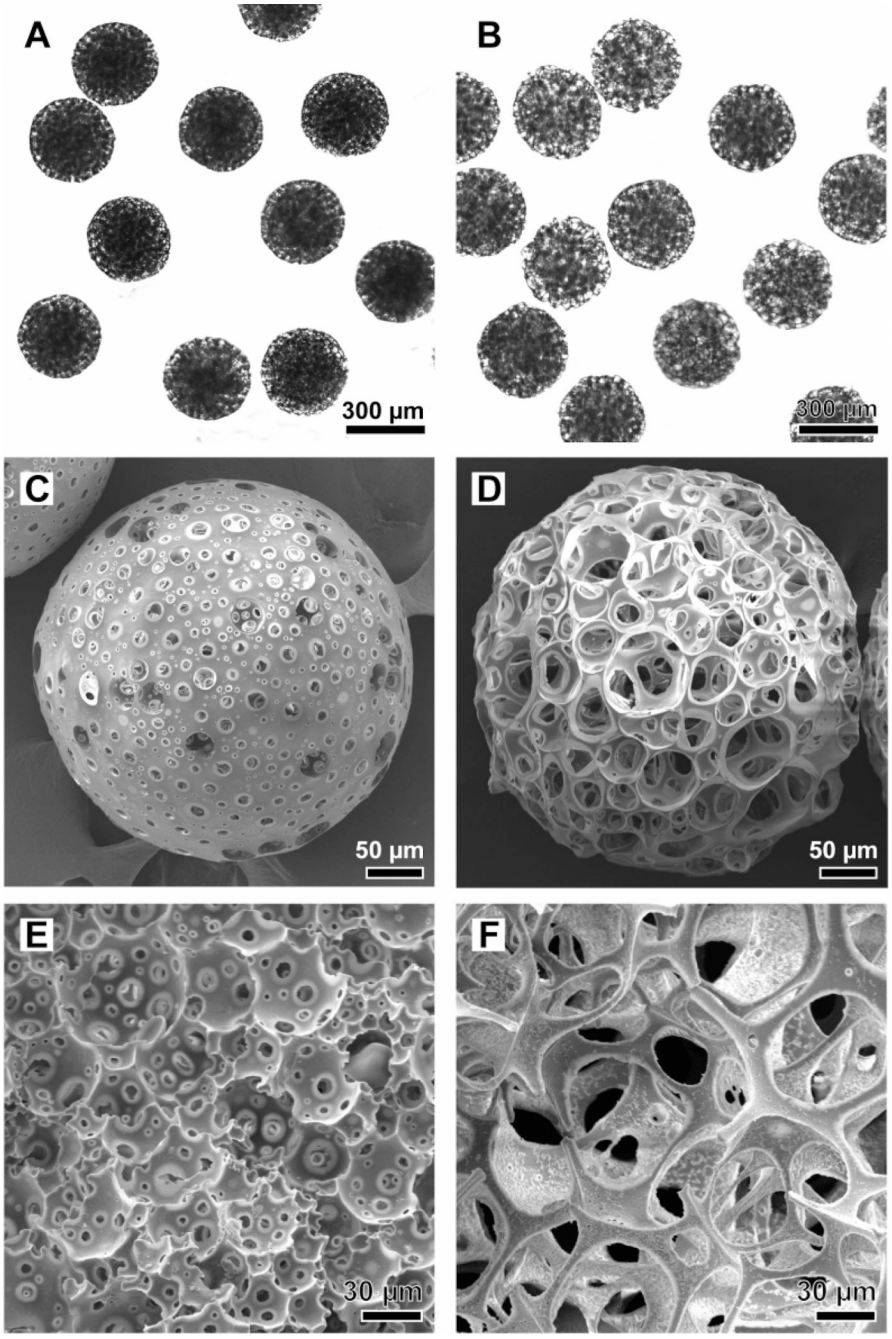

Figure 3.
A, B) Optical micrographs and C–F) SEM images of porous beads with A, C, and E) small and B, D, and F) large pores. E) and F) cross-sections of individual beads.

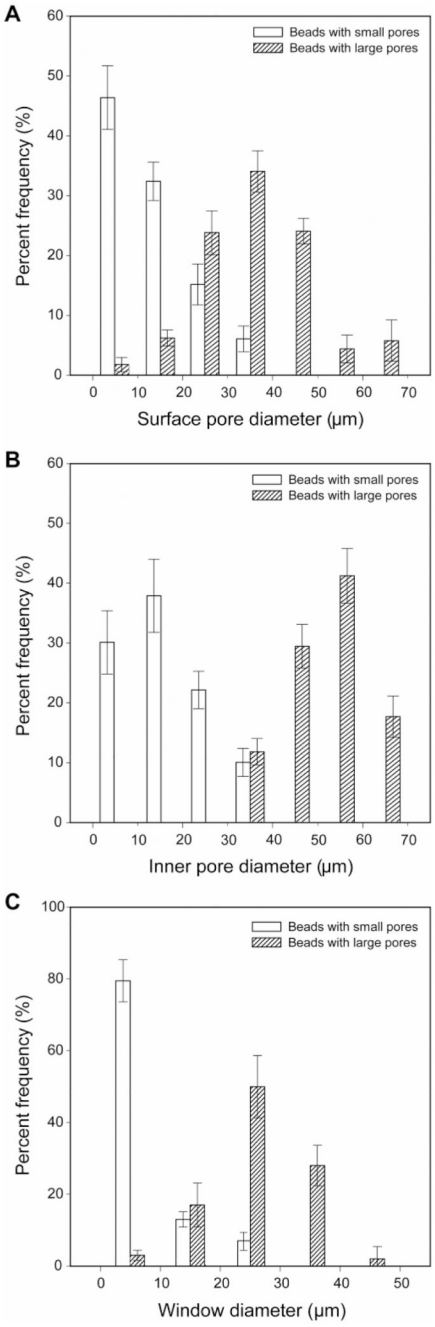

Figure 4.

Size distributions for A) surface pores, B) inner pores, and C) the windows connecting the inner pores for the beads with small and large pores. For each sample, at least 100 pores and windows from different 5 samples were analyzed.

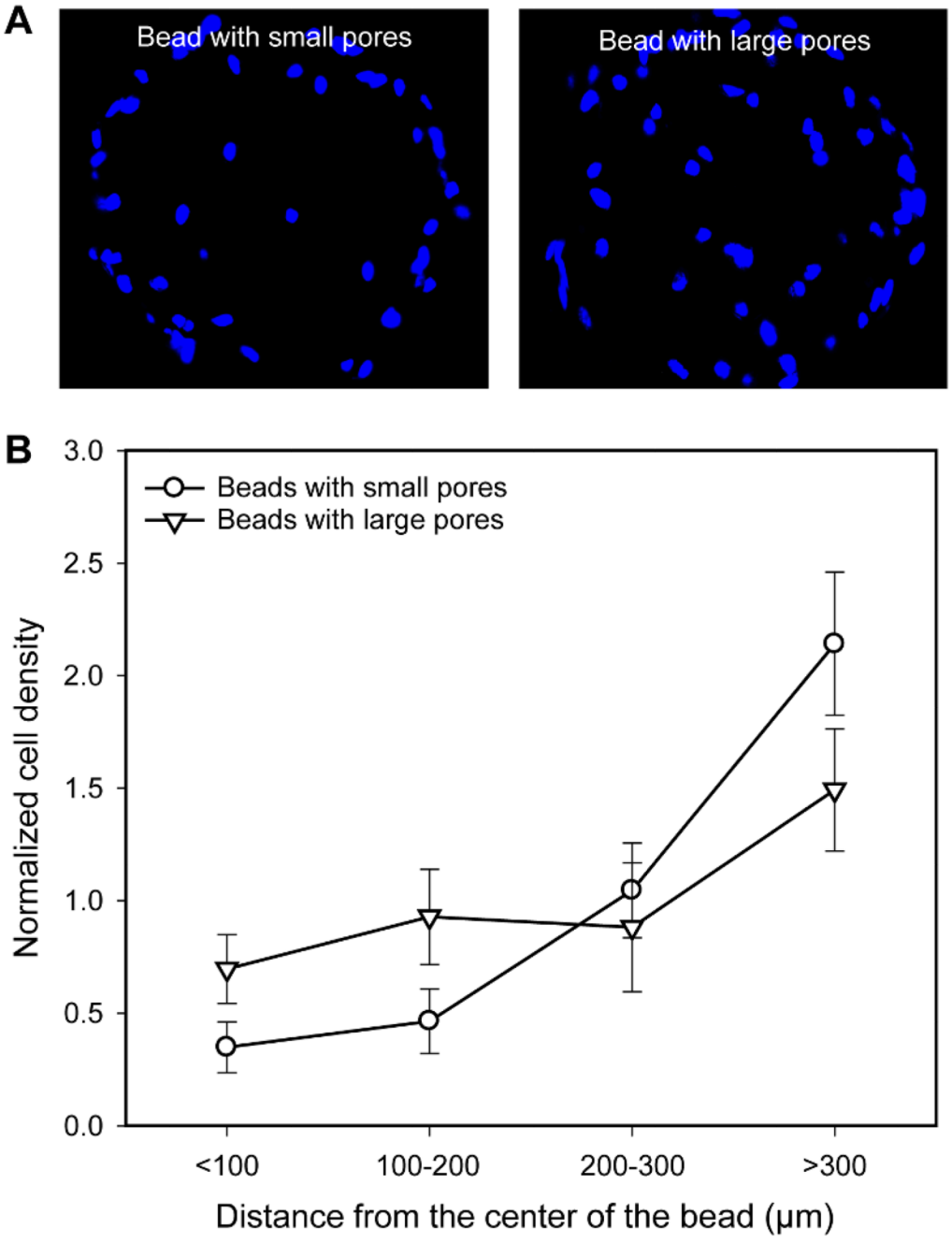

Figure 5.

A) Fluorescence micrographs taken from the microtomed samples (20 μm in thickness) obtained after 1 day of culture. The images were taken after nucleus staining. B) Normalized cell density in the beads with small and large pores as a function of the distance from the center of the bead (n = 3). All the data were normalized to the average cell density.

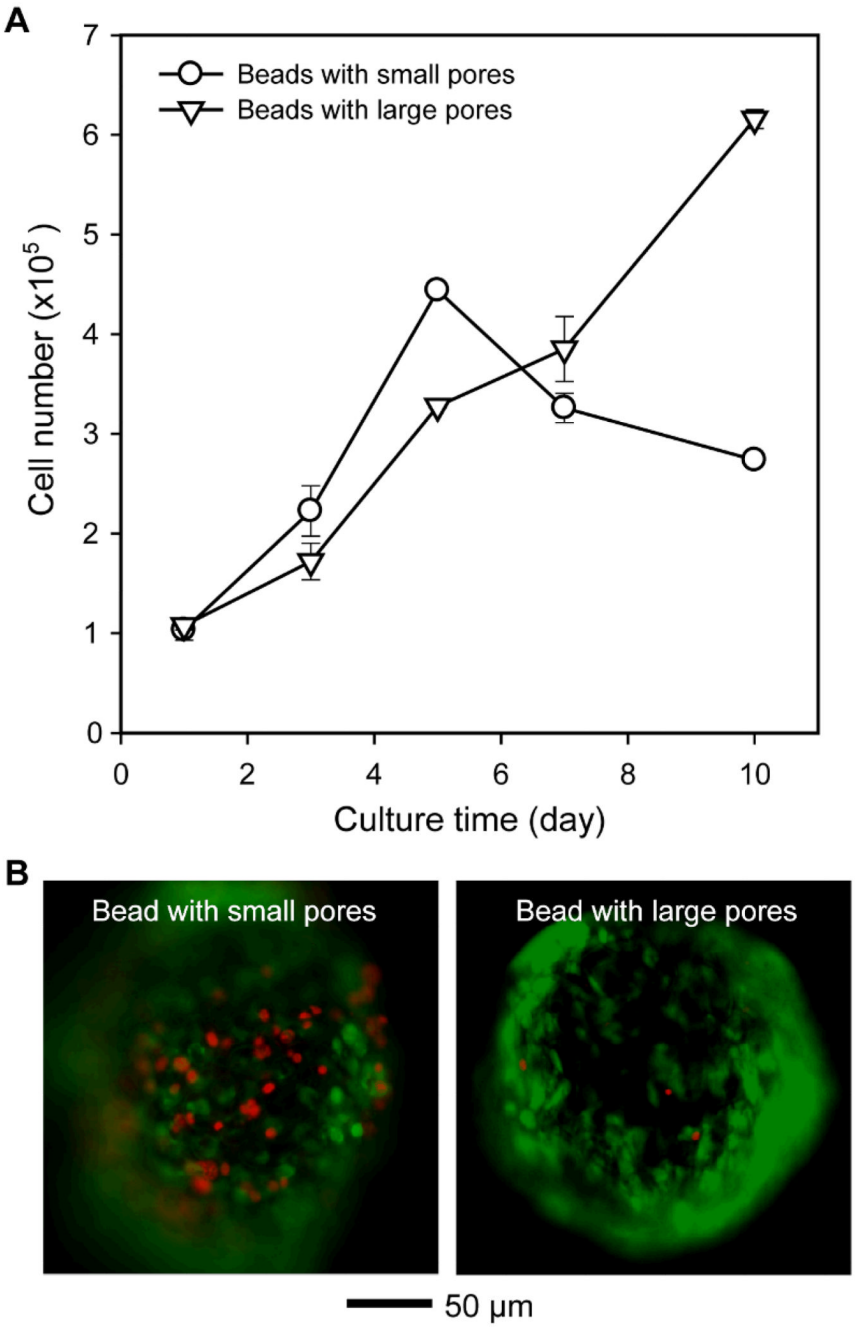

Figure 6.

A) Proliferation of fibroblast in the beads with small and large pores as a function of culture time (n = 3). B) Fluorescence micrographs of cells in the bead with small and large pores after 10 days of culture. Green and red colors in fluorescence micrographs indicate live and dead cells, respectively.

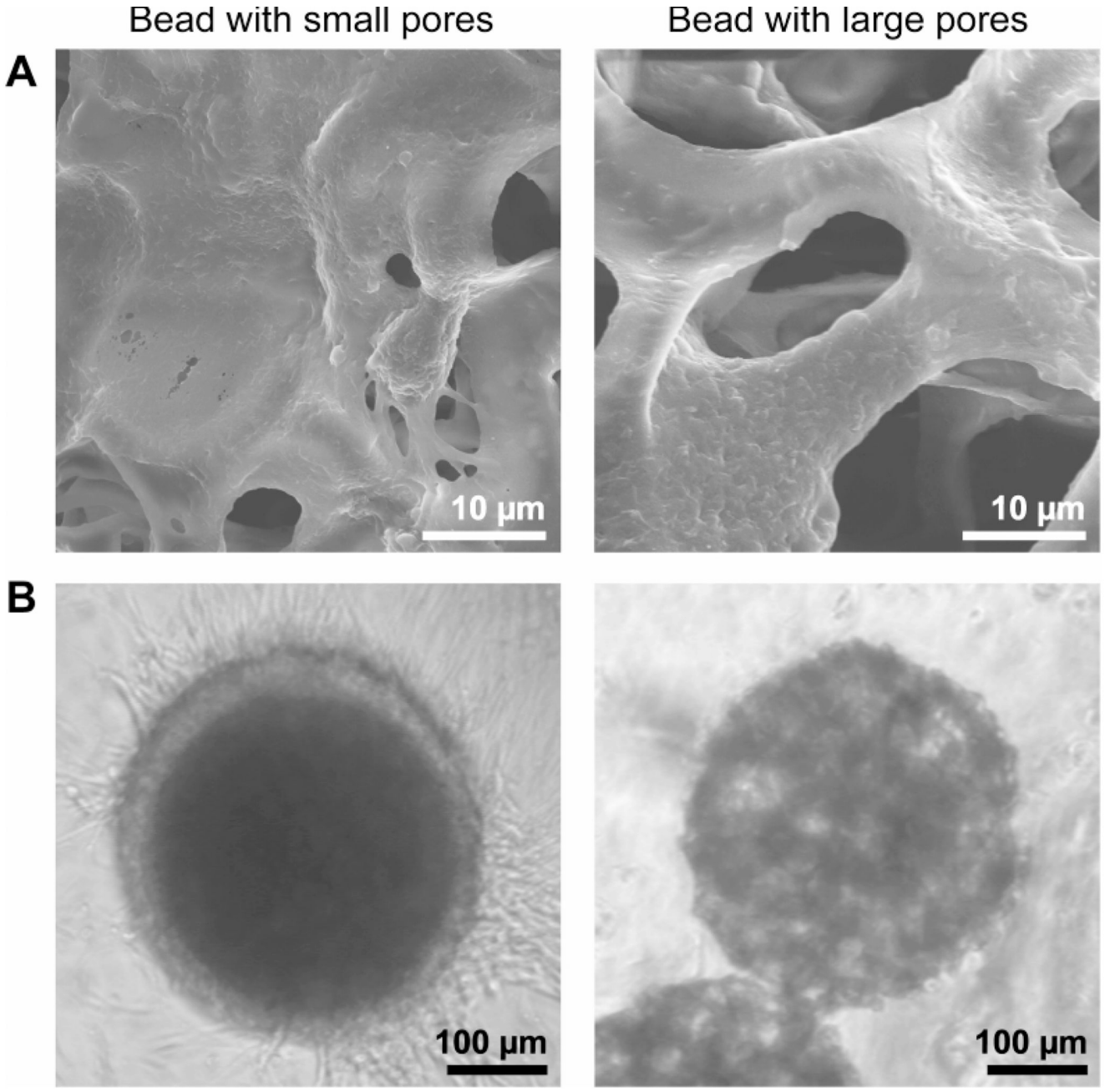

Figure 7.
A) SEM images taken from microtomed sample after culture for 1 day, and B) optical micrographs of the cell/bead construct after culture for 7 days.